

Jet Energy Loss in Hot and Dense Matter

I. Vitev¹, M. Gyulassy¹, and P. Levai²

¹ Department of Physics, Columbia University, 538 West 120-th Street,
New York, NY 10027, USA

² KFKI Research Institute for Particle and Nuclear Physics,
P.O. Box 49, Budapest 1525, Hungary

Abstract. We discuss the the GLV Reaction Operator formalism for computing the non-abelian energy loss of jets propagating through hot and dense matter. We incorporate our results on induced gluon bremsstrahlung together with the effects of nuclear shadowing and multiple scattering in a two component soft+hard description of heavy ion reactions at RHIC energies. We demonstrate that good agreement between data and theory can be achieved in the measured moderate $p_T < 5$ GeV window at $\sqrt{s} = 130$ AGeV and we extend our predictions for the high p_T part of the hadronic spectra. We focus on the perspectives of using jet tomographic methods for probing not only the density and geometry of the quark-gluon plasma but also its parton composition at various center of mass energies.

Keywords: non-abelian energy loss, jet tomography, partonic composition of the quark-gluon plasma

PACS: 12.38.Mh; 24.85.+p; 25.75.-q

1. Introduction

Coherent scattering effects on induced photon/gluon emission have been studied in both abelian and non-abelian gauge theories. Destructive interference of photon radiation from initially on-shell fast electrons propagating and multiply interacting in matter was first discussed by Landau and Pomeranchuk [1] and independently by Migdal [2]. Photon bremsstrahlung off asymptotically prepared jet states was found to be suppressed in the infrared ($\omega \rightarrow 0$) region relative to the naive Bethe-Heitler limit [3] of radiation resulting from independent collisions. Those results have been experimentally confirmed at SLAC [4].

The non-abelian generalization of Bethe-Heitler radiation was discussed by Bertsch and Gunion [5] in the presence of a single scattering center. In a QED-like scenario the case of multiple interactions was first investigated by Gyulassy

and Wang [6]. The non-abelian nature of QCD coherence was later employed by BDMPS [7] to show that in the high energy regime the mean energy loss of asymptotic jets is proportional to the square of the length of the medium, i.e. $\Delta E \sim L^2$. Those results were obtained for “thick” plasmas with a very large number of soft scatterings. Discussion of gluon bremsstrahlung in the path integral formalism can be found in Refs. [8, 9].

The GLV reaction operator approach [10] to non-abelian parton energy loss relies on a systematic expansion of induced gluon radiation associated with jet production in a dense QCD plasma in terms of correlations between multiple scattering centers. Analytic expressions for the induced inclusive gluon transverse momentum and light-cone momentum distributions are derived to all orders in powers of the opacity of the medium, $\chi = N\sigma_g/A = L/\lambda_g$. The analytic solution to all orders in opacity generalizes previous continuum results by allowing for arbitrary correlated nuclear geometry and evolving screening scales as well as the inclusion of finite kinematic constraints. In comparison to data we use numerical results corrected up to third order in χ that allow us to extend jet quenching computations down to parton energies $E \sim 5$ GeV. For gaining theoretical insight, however, it is useful to resort to analytic formulas that neglect some of the kinematic constraints but capture the essential features of parton energy loss. The dominant first order energy loss can be written as

$$\Delta E^{(1)} = \frac{C_R \alpha_s}{2} \int_{\tau_0}^{\infty} d\tau \frac{\mu^2(\tau)}{\lambda(\tau)} (\tau - \tau_0) \log \frac{2E}{\mu^2 L}, \quad (1)$$

where C_R is the second casimir in the representation of the jet and the $\mu^2(\tau)/\lambda(\tau)$ is the local “transport coefficient”. In a hot and dense medium in local thermal equilibrium $\mu^2(\tau) = 4\pi\alpha_s T^2(\tau)$ and perturbatively one can express $\mu^2(\tau)/\lambda(\tau) = (C_T C_A/d_A)4\pi\alpha_s^2 \rho(\tau)$, where C_T is the color charge of the target and d_A is the dimension of the adjoint representation. This formulation allows to account for the realistic dynamical time evolution of the systems created in ultra-relativistic nucleus-nucleus collisions.

Jet tomography is the QCD analog of conventional X-ray tomography that exploits the attenuation of high energy jets produced in nuclear matter [11]. We use the term “jet tomography”, inspired by a seminar by Istvan Lovas [12] entitled “Vector meson tomography of the QGP”, to contrast the particular advantages of high p_T PQCD probes of the density evolution of partonic matter formed in A+A reactions. The dependence of the non-abelian energy loss on the density and geometry of the medium as seen in Eq. (1) provides a rigorous theoretical framework for the jet tomographic analysis discussed in Refs. [13, 14, 15, 16, 17]. The experimental discovery of a factor of ~ 3 suppression of moderate $p_T \lesssim 4$ GeV π^0 's in central $Au + Au$ reactions by PHENIX [18] and the discovery of large transverse asymmetries in non-central collisions for $p_T \lesssim 5$ GeV by STAR [19] have confirmed that the high p_T frontier at RHIC does in fact provide a wide range of new physics opportunities.

We here present the results of our calculation of the suppression of high p_T

particle spectra relative to the binary collision scaled pp reference baseline and the p_T and centrality dependence of the p/π ratios [17]. We find good agreement between data and theory for jet energy loss driven by initial gluon rapidity density $dN^g/dy \simeq 800$. One of the descriptions of soft parton production, based on the saturation models [20], suggests slow variation of the number densities of quanta per unit rapidity achieved in the early stages of A+A reactions with \sqrt{s} and therefore a slow variation of the quenching factor. In contrast, at SPS energies moderate p_T neutral pions were found to be enhanced^a by a factor ~ 2 [21]. We propose that one possible solution to this puzzle may be related to differences in the composition of the non-abelian plasma (quarks vs. gluons), an important detail that has so far been ignored in jet tomographic studies.

2. Induced Gluon Radiation

The GLV formalism [10] for multiple elastic and inelastic interactions inside nuclear matter expands the differential probability of observing a final state jet or jet+gluon system (described by a set of quantum numbers $\{\alpha\}$) in orders of the correlations between multiple scattering centers, i.e. $P(\{\alpha\}) = \sum_n P^{(n)}(\{\alpha\})$. In the high energy eikonal approximation^b a major simplification occurs as a result of the well defined path ordering of sequential interactions inside the medium. It is therefore possible to build all relevant classes of amplitudes by subsequent insertion of single Born or “direct” (\hat{D}) and double Born or “virtual” (\hat{V}) interactions. At the probability level the recursion relation is generated by the reaction operator [10] $\hat{R} = \hat{D}^\dagger \hat{D} + \hat{V}^\dagger + \hat{V}$. The virtual corrections $\hat{V}^\dagger + \hat{V}$ to the naive elastic scattering component $\hat{D}^\dagger \hat{D}$ ensure unitarity in the GLV formalism. The approach described here is quite general, i.e. within the framework of the approximations stated for an arbitrary initial condition described by an amplitude A_0 , $P^{(n)}(\{\alpha\}) \propto A_0^\dagger (\hat{R})^n A_0$. The technical part of the calculation includes solving for the color and kinematic structure of the “direct” and “virtual” operators. Recently this was illustrated via a computation of the elastic broadening of jets propagating in nuclear matter [22].

For the case of jets produced at finite time t_0 in heavy ion reactions the solution for the double differential gluon radiation intensity was given in Ref. [10]

$$\begin{aligned} \frac{dI^{ind.}}{dx d^2\mathbf{k}} &= \frac{C_R \alpha_s}{\pi^2} \sum_{n=1}^{\infty} \prod_{i=1}^n \int_0^{L-\Delta z_1 \dots - \Delta z_{i-1}} \frac{d\Delta z_i}{\lambda_g(i)} \int (d^2\mathbf{q}_i [\bar{v}_i^2(\mathbf{q}_i) - \delta^2(\mathbf{q}_i)]) \times \\ &\times \left(-2 \mathbf{C}_{(1, \dots, n)} \cdot \sum_{m=1}^n \mathbf{B}_{(m+1, \dots, n)(m, \dots, n)} \times \right. \\ &\times \left. \left[\cos \left(\sum_{k=2}^m \omega_{(k, \dots, n)} \Delta z_k \right) - \cos \left(\sum_{k=1}^m \omega_{(k, \dots, n)} \Delta z_k \right) \right] \right), \quad (2) \end{aligned}$$

where $\mathbf{C}_{(1,\dots,n)} = \frac{1}{2}\nabla_{\mathbf{k}} \log(\mathbf{k} - \mathbf{q}_1 - \dots - \mathbf{q}_n)^2$, $\mathbf{B}_{(m+1,\dots,n)(m,\dots,n)} \equiv \mathbf{C}_{(m+1,\dots,n)} - \mathbf{C}_{(m,\dots,n)}$ are the Bertsch-Gunion terms [5], and $\omega_{(k,\dots,n)} = 1/(2xE|\mathbf{C}_{(k,\dots,n)}|^2)$ are the interference phases that produce the non-abelian analog of the LPM effect [1, 2]. The destructive interference pattern can be seen at a *differential level* in Eq. (2). In the calculation of the gluon bremsstrahlung we use a normalized color-screened Yukawa potential leading to $\bar{v}_i^2(\mathbf{q}_i) = \mu^2/(\pi(\mathbf{q}_i^2 + \mu^2)^2)$. One unexpected result was that the series in Eq. (2) converges very fast [10, 23]. Even more surprisingly, the first term was found to give the dominant contribution and by integrating over the transverse momentum \mathbf{k} and light-cone momentum fraction x of the gluon one recovers the result of Eq. (1). In computing the spectrum of gluons and the energy loss of jets we take into account numerically corrections up to third order in the opacity χ and the evolution of the density of the system due to the longitudinal Bjorken expansion.

3. Hadronic Spectra at Moderate to High p_T

The computed energy loss spectrum is employed in the calculation of the quenched spectrum of hadrons. A jet of flavor c and transverse momentum p_c produced in a hard PQCD scattering $a + b \rightarrow c + d$ is attenuated prior to hadronization by the radiative energy loss to $p_c^* = p_c(1 - \epsilon)$. This shifts the hadronic fragmentation fraction $z_c = p_h/p_c$ to $z_c^* = z_c/(1 - \epsilon)$.

The invariant distribution of hadrons reduced by the energy loss in $A + A$ collision at impact parameter \mathbf{b} is then given by

$$E_h \frac{dN_h^{AA}}{d^3p} = T_{AA}(\mathbf{b}) \sum_{abcd} \int dx_1 dx_2 d^2k_{T,a} d^2k_{T,b} g(\vec{k}_{T,a}) g(\vec{k}_{T,b}) f_{a/A}(x_1, Q^2) f_{b/A}(x_2, Q^2) \frac{d\sigma^{ab \rightarrow cd}}{d\hat{t}} \int d\epsilon P(\epsilon, p_c) \frac{z_c^*}{z_c} \frac{D_{\pi^0/c}(z_c^*, Q^2)}{\pi z_c}, \quad (3)$$

where $T_{AA}(\mathbf{b})$ is the Glauber profile density. The fragmentation functions $D_{h/c}(z, Q^2)$ is taken from BKK [24] and the structure functions for $f_{a/A}(x, Q^2)$ (we take the GRV94 LO [25]) include the isospin dependence. Nuclear shadowing, k_T broadening and Cronin effect are taken into account as in [26, 27, 28]. The modification of the fragmentation functions due to gluon radiation can be seen in Eq. (3) and is also discussed in [29]. The FFs carry the information of the medium induced jet energy loss but the observed suppression of high p_T is a result of the full calculation that folds in a variety of nuclear effects as well as the shape of the initial jet spectrum.

In order to extend our calculations to lower transverse momenta of hadrons we discuss a phenomenological soft component motivated by the string and baryon junction picture. We parametrize here this component as follows:

$$\frac{dN_s(\mathbf{b})}{dy d^2\mathbf{p}_T} = \sum_{\alpha=\pi, K, p, \dots} \frac{dn^\alpha}{dy}(\mathbf{b}) \frac{e^{-p_T/T^\alpha(\mathbf{b})}}{2\pi(T^\alpha(\mathbf{b}))^2}. \quad (4)$$

Such seemingly “thermal” distribution of hadrons is observed already in e^+e^- collisions and may be related to Gaussian fluctuations in the string tension [30]. As in string models the soft component is assumed to scale with the number of participants (N_{part}). In Eq. (4) we also account for the possibly different mean inverse slopes T^α for baryons and mesons. In the junction picture [31], the large T^B may arise from the predicted [32] smaller junction trajectory slope $\alpha'_J \approx \alpha'_R/3$. This implies that the *effective* string tension is three times higher than $1/(2\pi\alpha'_R) \approx 1$ GeV/fm leading in the massless limit to $\langle p_T^2 \rangle_J \simeq 3 \langle p_T^2 \rangle_R$. In terms of the string model the factor three enhancement of the mean square p_T is due to the random walk in p_T arising from the decay of the three strings attached to the junction. Naively, we would thus expect $T^B \simeq \sqrt{3} T^\pi$ predicting an approximately constant $\sqrt{\langle p_T^2 \rangle^B}$ for all baryon species.

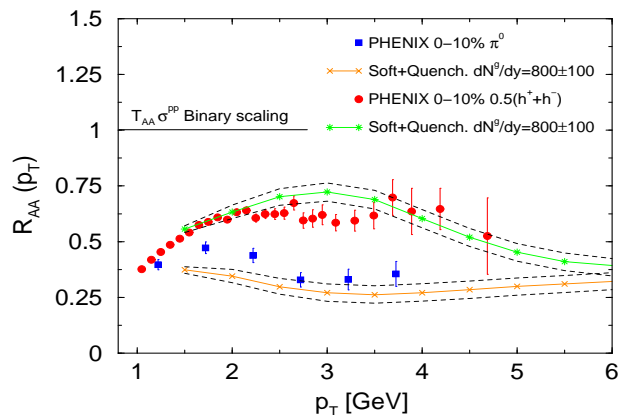


Fig. 1. The ratio of charged hadron and π^0 multiplicities to the binary collision scaled $\bar{p}p$ result is shown from [18]. The curves utilize the GLV quenched hard spectrum and the string and baryon junction soft component Eq. (4).

Fig. 1 shows the ratio R_{AA} of the differential particle yields relative to the binary collision scaled $\bar{p}p$ for inclusive charged hadrons and neutral pions. We obtain reasonable agreement with data if the jet energy loss is driven by initial gluon rapidity density $dN^g/dy \simeq 800$. This number is lower by $\sim 30\%$ from existing estimates. The difference in the suppression factor of π^0 and $0.5(h^+ + h^-)$ is understood through the possibly different baryon and meson production mechanisms in the moderate high $2 \leq p_T \leq 5$ GeV window. In our calculation pion production becomes PQCD dominated for $p_T > 2$ GeV and correspondingly suppressed by the jet energy loss. In contrast, baryon production in the region of interest is dominated through the junction mechanism by baryon transport in rapidity and moderate p_T . This accounts for the different suppression of neutral pions and inclusive charged hadrons as seen in Fig. 1. At large p_T baryon production also becomes perturbative, leading to a common suppression factor. This is manifest in the $p_T > 5$ GeV region of Fig. 1.

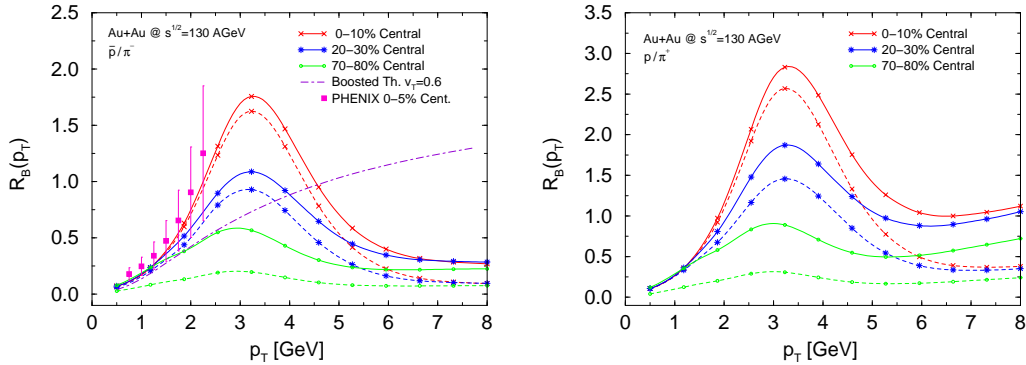


Fig. 2. The centrality dependence of p/π is predicted for three different centralities. Solid (dashed) lines correspond to A^1 ($A^{4/3}$) scaling of the baryon junction component. The ratio of \bar{p} and π^- fits to PHENIX data on central reactions is shown for comparison. A boosted thermal source (dashed line) is also shown. The left/right panel reflects negative/positive hadrons.

The interplay between soft and hard physics at RHIC is possibly most clearly seen in the p_T differential baryon/meson (R_B) ratios. Our predictions for the centrality and the p_T dependence of \bar{p}/π^- and p/π^+ are given in Fig. 2. An extended discussion can be found in Refs. [17, 33]. In central collisions the interplay between the anomalous baryon component and the quenched PQCD component of pions leads to maximum of R_B near $p_T \sim 3 - 4$ GeV/c. At large $p_T \geq 5 - 6$ GeV/c we predict a gradual decrease of R_B below unity consistent with the the PQCD baseline calculations [17]. In Fig. 1 we have included through error bands the factor of ~ 3 uncertainty in the fragmentation functions into \bar{p}, p at high p_T . The solid and dashed curves reflect the difference between the N_{part} and $N_{part}^{4/3}$ scaling of the junction component.

In peripheral reactions the size of the interaction region as well as the initial density of the medium decrease, leading to a reduction of energy loss. The absence of quenching reduces the observability of the anomalous component and the p/π ratio may stay below unity for all p_T . The case of peripheral reactions is hence similar to $\bar{p}p$ collisions. The experimentally testable prediction of the model is therefore that the maximum of the $R_B = p/\pi$ ratio decreases with increasing impact parameter, decreasing participant number, or equivalently decreasing dN^{ch}/dy . The reduction of R_B at large p_T is also an important prediction of our computation and is not seen by other models attempting fits only in regions of p_T where experimental data already exists.

4. Jet Tomography of the QGP Partonic Composition

Two extreme scenarios for the composition of the quark-gluon plasma have been extensively discussed in the literature. In one scenario, based on saturation models [34], the hot and dense matter created in A+A collisions is interpreted as purely gluonic degrees of freedom. Alternatively, quark coalescence models [35] advocate the creation of dense quark-antiquark matter as a result of the very fast decay of *massive* gluons into quark degrees of freedom [36]. We here propose that jet tomography is a powerful tool that can distinguish between different scenarios.

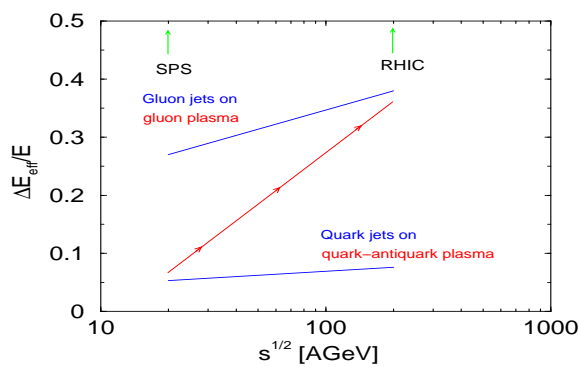


Fig. 3. The *effective* fractional energy loss for $E = 6$ GeV jet is plotted versus \sqrt{s} for two extreme scenarios.

Fig. 3 illustrates the idea behind the QGP composition tomography. We contrast the case of gluon jets propagating through gluon plasma to the case of quarks propagating through quark-antiquark plasma at center of mass energies ranging from $\sqrt{s} = 20$ AGeV at SPS to $\sqrt{s} = 200$ AGeV (the top RHIC energy). The variation in the effective fractional energy loss (using an approximately constant density renormalization factor $Z \simeq 0.4 - 0.5$ [23]) is small $\sim 50\%$ due to the small change of the initial density of quanta per unit rapidity (this can be most easily seen from the naive picture of parton-hadron duality). In contrast, the changing plasma composition and the jet representation lead to a factor of $(C_A/C_F)^2 \simeq 5$ difference. While neither of the extreme scenarios may hold for the broad range of collision energies in question, it is possible that the partonic composition of the system created in heavy ion reactions evolves as a function of \sqrt{s} , leading to pronounced differences in $\Delta E_{eff}(\sqrt{s})/E$ as indicated in Fig. 3. Faster than expected increase of energy loss with T/T_c was also discussed in a Polyakov Loop model [38].

The quenching of neutral pions is shown in Fig. 4. In this particular example we study only the effect of energy loss and we have not included nuclear shadowing and Cronin effect. We have also not included a phenomenological soft component to mock the part of phase space that is not perturbatively accessible and is possibly

sensitive to higher twist effects. In Fig. 4 the medium that drives the quenching of high p_T jets at RHIC $\sqrt{s} = 130$ AGeV is reinterpreted as composed of 60% gluons and 40% quarks and antiquarks. At $\sqrt{s} = 200$ AGeV Au+Au the number of quanta per unit rapidity increases only by $\sim 15\%$ [37]. The dashed line illustrates the suppression factor R_{AA} for this slightly increased rapidity density of soft partons when unchanged QGP composition is assumed. We note that the effect is even smaller than naively expected ($\sim 15\%$) due to finite kinematics effects in computing $\Delta E/E$ and hadronization. Detectable increase $\sim 30\%$ in the π^0 suppression factor is only possible if one assumes a transition to almost completely gluon dominated soft background as shown in Fig. 4.

At smaller center of mass energies ($\sqrt{s} = 20$ AGeV) we have studied the case of jets propagating through quark-antiquark plasma. We have used phenomenologically a smaller mean energy loss renormalization coefficient $Z = 0.2$ to account for the possibly bigger energy loss fluctuations (more detailed studies of Z are needed). Those effects tend to strongly reduce the effective energy loss. The observed suppression factor R_{AA} , however, convolutes the apparent decrease of $\Delta E_{eff}/E$ with the much steeper p_T differential hadron distributions (3). As a result a still significant suppression of neutral pions ($R_{AA} \sim 0.5$) remains, which is inconsistent with the current SPS results [21]. It is important to improve the jet tomographic calculation presented in Fig. 4 to take into account Cronin effect and nuclear (anti)shadowing in a more quantitative comparison to the WA98 data as well as to investigate the cause for the unusually small energy loss at SPS.

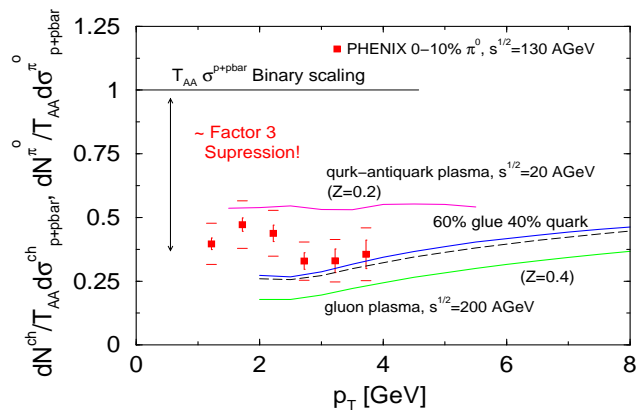


Fig. 4. The π^0 suppression factor resulting from the non-abelian energy loss of jets is shown.

5. Conclusions

We have shown that in a two component soft+hard model that incorporates jet energy loss computed in the GLV formalism [10] one can account for the suppression of the inclusive charged hadrons and neutral pions seen in the $\sqrt{s} = 130$ AGeV RHIC

run. Jet tomography is shown to be an important probe of the partonic composition of the hot and dense medium created in the initial stages of heavy ion reactions. In particular, at CERN SPS energy of $\sqrt{s} \sim 20$ AGeV large energy loss induced by *gluon* medium on *gluon* jets seems excluded by data.

Acknowledgements

We are grateful to MTA academician I. Lovas for inspiring discussions on the importance of tomographic analysis of A+A reactions, and we celebrate his 70th birthday. Discussions with MTA septarian academicians J. Zimanyi and J. Nemeth throughout many years are also gratefully acknowledged on the occasion of their mutual birthdays. This trio of nuclear theorists have advanced nuclear physics worldwide and we wish them an equally productive future. This work was supported by the Director, Office of Science, Office of High Energy and Nuclear Physics, Division of Nuclear Physics, of the U.S. Department of Energy under Contract No. DE-FG02-93ER40764 and by the U.S. NSF under INT-0000211 and OTKA No. T029158.

Notes

- a. Recent reanalysis of the WA98 data (M.M. Aggarwal *et al.*, Eur. Phys. J. **C23**, 225 (2002).) suggests that the enhancement estimates should be reduced by $\sim 30\%$.
- b. All recent approaches [7, 8, 9, 10] that discuss the LPM effect in QED and QCD employ the eikonal approximation together with a model of well separated scattering centers $\mu\lambda \gg 1$. For the case of A+A reaction this condition sets a natural upper limit on the opacity χ of a medium of finite small size $L \sim 5$ fm and is suggestive of the dominant role of low order correlations between multiple scatterings as demonstrated by GLV [10].

References

1. L.D. Landau and I.J. Pomeranchuk, Dokl. Akad. Nauk. SSSR **92** 92 (1953).
2. A.B. Migdal, Phys. Rev. **103**, 1811 (1956).
3. H.A. Bethe and W. Heitler, Proc. Royal Soc. **A146**, 83 (1934).
4. S. Klein, Rev. Mod. Phys. **71**, 1501 (1999); P.L. Anthony *et al.*, Phys. Rev. Lett. **76**, 3550 (1996).
5. J. F. Gunion and G. Bertsch, Phys. Rev. **D25**, (1982) 746.
6. M. Gyulassy and X.N. Wang, Nucl. Phys. **B420**, 583 (1994); X.-N. Wang, M. Gyulassy and M. Plumer, Phys. Rev. **D51**, 3436 (1995).
7. R. Baier, Yu.L. Dokshitzer, A.H. Mueller, S. Peigné and D. Schiff, Nucl. Phys. **B484**, 256 (1997).
8. B.G. Zakharov, JETP Lett. **73**, 49 (2001).
9. U.A. Wiedemann, Nucl. Phys. **B588**, 303 (2000).

10. M. Gyulassy, P. Levai, I. Vitev, Nucl. Phys. **B571**, 197 (2000); Nucl. Phys. **B594**, 371 (2001); Phys. Rev. Lett. **85**, 5535 (2000).
11. M. Gyulassy, 40th Internationale Universitatswochen Fuer Theoretische Physik: Dense Matter (IUKT 40), nucl-th/0106072.
12. I. Lovas, Collegium Budapest Workshop, Budapest March 27, 2001; see also these proceedings.
13. M. Gyulassy, I. Vitev, X.-N. Wang, Phys. Rev. Lett. **86**, 2537 (2001).
14. P. Levai, G. Papp, G. Fai, M. Gyulassy, G. G. Barnafoldi, I. Vitev and Y. Zhang, Nucl. Phys. **A698**, 631 (2002).
15. G. Fai, G. G. Barnafoldi, M. Gyulassy, P. Levai, G. Papp, I. Vitev and Y. Zhang, International Europhysics Conference On High-Energy Physics (HEP 2001), hep-ph/0111211.
16. M. Gyulassy, I. Vitev, X.N. Wang, P. Huovinen, Phys. Lett. **B526**, 301 (2002).
17. I. Vitev and M. Gyulassy, nucl-th/0104066, Phys. Rev. C in press.
18. K. Adcox *et al.*, Phys. Rev. Lett. **88**, 022301 (2002) ; G. David *et al.*, Nucl. Phys. **A698**, 227 (2002).
19. K.H. Ackermann *et al.*, Phys. Rev. Lett. **86**, 402 (2001); C. Adler *et al.*, Phys. Rev. Lett. **87**, 182301 (2001).
20. K.J. Eskola, K. Kajantie, P.V. Ruuskanen, K. Tuominen, Nucl. Phys. **B570**, 379 (2000).
21. X.-N. Wang, Phys. Rev. Lett. **81**, 2655 (1998).
22. M. Gyulassy, P. Levai and I. Vitev, arXiv: nucl-th/0201078.
23. M. Gyulassy, P. Levai and I. Vitev, arXiv: nucl-th/0112071.
24. J. Binnewies, B.A. Kniehl and G. Kramer, Z. Phys. **C65**, 471 (1995).
25. M. Glück, E. Reya and W. Vogt, Z. Phys. **C67**, 433 (1995).
26. X.N. Wang, Phys. Rev. **C61**, 064910 (2000).
27. G. Papp, P. Lévai, G. Fai, Phys. Rev. **C61**, 021902 (2000).
28. Y. Zhang, G. Fai, G. Papp, P. Lévai, G.G. Barnaföldi, Phys. Rev. **C65** 034903 (2002).
29. E. Wang and X.N. Wang, arXiv: hep-ph/0202105.
30. A. Bialas, Phys. Lett. **B466** 301 (1999).
31. G.C. Rossi and G. Veneziano, Nucl. Phys. **B123** 507 (1977).
32. D. Kharzeev, Phys. Lett. **B378** 238 (1996); S.E. Vance, M. Gyulassy, X.-N. Wang, Phys. Lett. **B443** (1998) 45; S.E. Vance, M. Gyulassy, Phys. Rev. Lett. **83** (1999) 1735.
33. I. Vitev, M. Gyulassy and P. Levai, International Europhysics Conference on High-Energy Physics (HEP 2001), hep-ph/0109198; I. Vitev, M. Gyulassy, International Nuclear Physics Conference (INPC 2001), hep-ph/0108045.
34. Y. Kovchegov, Nucl. Phys. **A692**, 557 (2001).
35. J. Zimanyi, T.S. Biro, T. Csorgo and P. Levai, Phys. Lett. **B472** 243 (2000).
36. P. Levai and U. Heinz, Phys. Rev. **C57** 1879 (1998).
37. B.B. Back *et al.*, arXiv: nucl-ex/0201005
38. A. Dumitru, R.D. Pisarski, Phys. Lett. **B525** 95 (2002).